Manuscript: An unusual clast in lunar meteorite MacAlpine Hills 88105: a unique lunar sample or projectile debris?

Authors: K. H. Joy, I. A. Crawford, G. R. Huss, K. Nagashima, and G. J. Taylor

Journal: Meteoritics and Planetary Science

Manuscript Number: MAPS-1968

Associate Editor: Dr. Cyrena Goodrich

An unusual clast in lunar meteorite MacAlpine Hills 88105: a unique lunar sample or projectile debris?

K. H. Joy[1], I. A. Crawford[2,3], G. R. Huss[4], K. Nagashima[4], G. J. Taylor[4]

[1]School of Earth, Atmospheric and Environmental Sciences, University of Manchester, Williamson Building, Oxford Road, Manchester, M13 9PL, UK.

[2]Dept. of Earth and Planetary Sciences, Birkbeck, University of London, Malet Street, Bloomsbury, London WC1E 7HX.

[3]The Centre for Planetary Sciences at UCL/Birkbeck, Gower Street, London, WC1E 6BT, UK.

[4]Hawai‘i Institute of Geophysics and Planetology, School of Ocean and Earth Science and Technology, University of Hawai‘i at Mānoa, 1680 East-West Road, Honolulu, HI 96822, USA.

Corresponding author: katherine.joy@manchester.ac.uk

Keywords: lunar-meteorite, lunar-regolith

Proposed running header: An unusual clast in lunar meteorite MacAlpine Hills 88105

Abstract

Lunar meteorite MacAlpine Hills (MAC) 88105 is a well-studied feldspathic regolith breccia dominated by rock and mineral fragments from the lunar highlands. Thin section MAC 88105,159 contains a small rock fragment, 400 × 350 µm in size, which is compositionally anomalous compared with other MAC 88105 lithic components. The clast is composed of olivine and plagioclase with minor pyroxene and interstitial devitrified glass component. It is magnesian, akin to samples in the lunar High-Mg Suite, and also alkali-rich, akin to samples in the lunar High-Alkali Suite. It could represent a small fragment of late-stage interstitial melt from an Mg-Suite parent lithology. However, olivine and pyroxene in the clast have Fe/Mn ratios and minor element concentrations that are different from known types of lunar lithologies. As Fe/Mn ratios are notably indicative of planetary origin, the clast could either (i) have a unique lunar magmatic source, or (ii) have a non-lunar origin (i.e., consist of achondritic meteorite debris that survived delivery to the lunar surface). Both hypotheses are considered and discussed.

1. Introduction

The lunar regolith is an important boundary layer between the Moon and the surrounding space environment (Hörz et al., 1991; McKay et al., 1991; Lucey et al., 2006). At any one locality the lunar regolith typically contains a record of diverse rock types (Korotev et al., 2003), mixed vertically and laterally by impacts, and material added to the Moon by projectiles (see Joy et al., 2012 for a summary). Interactions with the solar wind (Wieler, 1998) and the galactic environment (Crawford et al., 2010) further modify the regolith.

58 Lunar regolith breccias (Fruland, 1983) are rocks formed when the regolith was consolidated by pressure
59 (e.g., shock, overburdening) and/or thermal sintering. They, therefore, provide a random global sampling
60 of consolidated regolith from the Moon. These samples are not thought to have been fused by the impact
61 cratering event that ejected them from the lunar surface into Earth-crossing orbits, because many of them
62 have high trapped $^{40}Ar/^{36}Ar$ ratios, thought to be an indicator of sample antiquity (McKay et al. 1986;
63 Eugster et al., 2001; Joy et al., 2011a). This suggests that they represent examples of lithified
64 palaeoregoliths from different times in the Moon's past. Regolith breccias are, thus, time-capsules: once
65 they are consolidated into rocks they preserve a record of ancient lunar and Solar System processes.
66 Temporally constraining this archive sheds light on different times in the Moon's past, helping to better
67 understand the geological history of the Moon itself (McKay et al., 1986; Joy et al., 2011a), and the
68 bombardment history of the Moon, Earth and Solar System (Joy et al., 2012).

69

70 We present here results from the serendipitous discovery of a compositionally unusual clast found in
71 lunar meteorite MacAlpine Hills (MAC) 88105 and discuss its possible origin. MAC 88105, and its
72 paired stone MAC 88104, are feldspathic polymict regolith breccias (Lindstrom et al., 1991; Jolliff et al.,
73 1991; Koeberl et al., 1991; Neal et al., 1991; Warren and Kallemeyn, 1991). The meteorites are composed
74 of clasts of anorthositic igneous rocks, metaclastic granulitic clasts, impact glass and melt (Delano, 1991;
75 Taylor, 1991; Cohen et al., 2005; Joy et al., 2010a), and rare mare basalt fragments (Robinson et al.,
76 2012) consolidated by a fine-grained glassy melt matrix. The MAC 88104/05 samples have bulk
77 compositions similar to present day regoliths in the Outer-Feldspathic Highlands Terrane (FHT-O),
78 including the south polar highlands area, highlands south of Tycho crater, farside far northern highlands,
79 and feldspathic terranes surrounding Mare Australe (see Fig. 11d of Joy et al., 2010a).

80

2. Sample and Methods

We were allocated a thick (100 µm) section, MAC 88105,159, by the Meteorite Working Group. The section is approximately 12 × 6 × 0.1 mm in size. We have previously analysed the mineral chemistry of impact melt breccia clasts in the sample, and these results were published by Joy et al. (2010a). Additional mineral chemistry data is also presented here from phases in the MAC 88104,47, MAC 88105,158 and MAC 88104,48 sections. The samples were carbon coated and analysed using the London Natural History Museum's (NHM) JEOL 5900 LV SEM fitted with an Oxford Instruments INCA energy dispersive spectrometer (EDS) X-ray microanalyzer system (20 KV, 2 nA, 1 µm beam). This technique was used to collect back-scatter electron (BSE) and false colour element maps of the MAC 88105,159 section that are shown in Figure 1. Mineral chemistry was analysed using the NHM Cameca SX 50 electron microprobe (EMP, 20 KV, 20 nA, 1 µm beam), following the instrument setup described in full by Joy et al. (2010a). Data were checked for mineral stoichiometry and only data with analytical totals of between 97 and 102 % were accepted (see Electronic Appendix).

We also measured olivine and pyroxene mineral chemistries using the NASA Johnson Space Center Cameca SX 100 EMP instrument using a 1 µm beam, an accelerating voltage of 20 KV and a beam current of 40 nA following the method used by Joy et al. (2012). Long count times (200-300 secs) were employed on the Mn, Ni and Co peaks, and Co was corrected for the Fe K-β, Co K-α peak overlap. Elements were standardised to natural mineral standards and pure metals. For these high beam current settings the detection limits were ~63 ppm for Mn, ~77 ppm for Co and ~80 ppm for Ni. There is good agreement between the data acquired from the NHM and JSC Cameca SX 50 instruments (Table EA S1).

We measured 41 elements in a plagioclase grain, an olivine grain and in the bulk mesostasis of the clast by laser ablation inductively coupled plasma mass spectrometry (LA-ICP-MS) using an *Agilent* 7500a quadrupole system at University College London (UCL). We operated the *New Wave* aperture imaged frequency quintupled Nd:YAG laser ablation system (213 nm) laser source with a pulse frequency of 20 Hz set at 75% efficiency, and with a spot size of 55 µm. Background conditions were monitored for 1 minute and the sample was ablated for 30 seconds. Data were reduced using the GEMOC Glitter software (http://www.glitter-gemoc.com/), where plots of counts per second versus time were examined for each element per analysis, and integration intervals for the gas background and the sample analysis were selected manually.

Analyses were calibrated with NIST 612 external standard measurements (a synthetic doped glass; Pearce et al., 1997) using the same instrument setup. Calcium (^{42}Ca) was used as an internal standard for the plagioclase and mesostasis analyses, using CaO abundance in clasts determined by EMP analysis (Table 1). For the olivine grain, we assessed the suitability of which element is an appropriate internal standard. We considered using ^{42}Ca (85262 ppm in NIST 612; Pearce et al., 1997), ^{47}Ti (48.11 ppm in NIST 612; Pearce et al., 1997) and ^{55}Mn (38.43 ppm in NIST 612: Pearce et al., 1997) as these three elements are measured with both the EMP and the LA-ICP-MS. NIST 612 (8.4 wt% Ca) is not a good matrix match for lunar olivine (typically <0.2 wt% Ca) and using it with ^{42}Ca for internal normalisation results in low trace element concentrations (Table EA S2). The concentration of ^{55}Mn in NIST 612 is also not a good match for lunar olivine (which typically has >700 ppm Mn: *e.g.*, Papike et al., 1998; Shearer and Papike, 2005; Schnare et al., 2008; Fagen et al., 2013) and using it for internal normalisation results in high trace element concentrations (Table EA S2; note also unrealistically high Ca abundances of ~7 wt%). ^{47}Ti has the most similar concentrations in the NIST 612 standard to lunar olivine (typically 40-400 ppm Ti,

127 occasionally up to 1000 ppm Ti) and so we selected it as the element best suited to act an internal LA-
128 ICP-MS standard when using NIST 612 as the external standard for olivine analysis.

129

130 When using ^{42}Ca as the internal standard, repeatability of the NIST 612 external standard measurements
131 has a total relative standard deviation range of between 0.7 and 7% for all elements analysed and was on
132 average 3.5%. Accuracy was assessed by comparing our repeat NIST 612 measurements to the Pearce et
133 al. (1997) NIST 612 values, where the percentage relative difference had a range of between 0.58 and
134 8.56 % and an average of 2.6%. When using ^{47}Ti as the internal standard, repeatability of the NIST 612
135 standard measurements has a total relative standard deviation range of between 1.5 and 7% for all
136 elements analysed and was on average 3.6%. Accuracy was assessed by comparing our repeat NIST 612
137 measurements to the Pearce et al. (1997) NIST 612 values, where the percent error relative difference had
138 a range of between 0.15 and 16 % and on average 10.3%. Reported errors (Table 1) are one sigma as
139 calculated by the Glitter software.

140

141 Oxygen isotope compositions were analyzed *in situ* with the University of Hawai‘i Cameca ims-1280 ion
142 microprobe using a technique similar to that described by Makide et al. (2009) and Joy et al. (2012*)*. A
143 400 pA focused Cs^+ primary ion beam was rastered over a 7 × 7 μm^2 area for 100 s to remove carbon
144 coating and any surface contaminants. Then the raster was reduced to 5 × 5 μm^2 and data were collected.
145 The secondary ion mass spectrometer was operated at −10 keV with a 50 eV energy window. Three
146 oxygen isotopes were collected using multicollection mode. $^{16}O^-$ was measured on a Faraday cup, while
147 $^{17}O^-$ and $^{18}O^-$ were measured with electron multipliers. The mass resolving power for $^{16}O^-$ and $^{18}O^-$ was
148 ~2000, and that for $^{17}O^-$ was ~6000, sufficient to separate interfering $^{16}OH^-$. A normal-incidence electron
149 flood gun was used for charge compensation.

Oxygen isotope analyses are reported in standard δ notation where $\delta^{18}O$ has been calculated as: $\delta^{18}O = (([^{18}O_{sample}/^{16}O_{sample}]/[^{18}O_{ref}/^{16}O_{ref}])-1) \times 1000$, and similarly for $\delta^{17}O$ using $^{17}O/^{16}O$ ratio. $\Delta^{17}O$ (deviation from the terrestrial fractionation line) is calculated as $\delta^{17}O - 0.52 \times \delta^{18}O$.

Terrestrial standards (San Carlos olivine and Miyakejima anorthite) were used to set up the instrument and check reproducibility of our measurement protocol. In order to minimise any possible differences in instrumental effects associated with different sample mounts, we analysed lunar plagioclase grains in the host MAC 88105,159 rock as an internal standard. The weighted mean of $\Delta^{17}O$ on lunar plagioclase measurements was assumed to be $\Delta^{17}O = 0$, and data for the clast are reported relative to the lunar plagioclase. In order to verify the positions of the sputtered region, the phases studied for oxygen isotopes were imaged in secondary and backscattered electrons using the University of Hawai‘i JEOL 5900LV scanning electron microscope after ion probe measurements.

3. Results

The MAC 88105,159 section is composed of a feldspathic regolith breccia with impact melt breccia clasts, anorthositic clasts and rare basalt and granitic lithologies (Fig. 1, see also Joy et al. 2010a). We identified a magnesian lithic clast (Fig. 2) as being compositionally distinct (Mg-rich and K-rich) in a false-colour element map of the sample (Fig. 1b). The clast is 400 × 350 µm in size and is transected by a 50-80 µm wide fracture that also cross-cuts the surrounding matrix (Fig. 2). The clast has a hypocrystalline texture (crystals within a glassy mesostasis groundmass) and is fine grained. It is

172 composed of blocky subhedral olivine and plagioclase crystals trapping elongate xenomorphic pyroxenes
173 and a late-stage glassy mesostasis (Fig. 2). There are no particles of Fe-metal present that would be
174 indicative of an impact melt origin. Modal abundances of minerals by mode were determined using
175 analysis of BSE and element map images (following the methods outlined in Snape et al., 2011) and these
176 phase proportions (Fig. 2c) indicate that the clast is an olivine-gabbro. However, given the small size of
177 the clast, this may not be representative of the parent lithology from where it was sourced. Mineral trace
178 elements measured in the clast are plotted in Figure 3, and major and minor element data are plotted in
179 Figures 4 to 8.

180

181 3.1 Mineral Chemistry Results

182

183 The clast has ~30 % (by area) zoned forsteritic olivine grains (Fo_{83-93}: Table EA S1). Olivine has Ni at
184 concentrations of <160 ppm (by EMP analysis, often less than detection limits of ~80 ppm: Table EA S1).
185 Concentrations of other minor elements in olivine are plotted in Figure 6 compared with a wide range of
186 olivine in lunar meteorites and Apollo samples. Olivine grains in the clast have higher Cr concentrations
187 (0.07-0.28 wt% Cr_2O_3: Fig. 6) and marginally higher CaO (0.15-0.44 wt%) and Ti (~170-1000 ppm) than
188 lunar samples with similar Mg-rich olivine (i.e., those from the Mg-Suite and KREEP basalts: Papike et
189 al., 1998; Shervais and McGee, 1998; Taylor et al., 2012).

190

191 Approximately 42 % (by area) of the clast is zoned blocky plagioclase ($An_{72-82,}$ where An# = atomic
192 Ca/[Ca+Na+K]; Mg# = 59-81, where Mg# = atomic 100×Mg/[Mg+Fe]; Table EA S3). Plagioclase grains
193 have a positive Eu-anomaly (Eu/Eu* = 6.6 where Eu/Eu* is calculated as $Eu_{cn}/\sqrt{[Sm_{cn} \times Gd_{cn}]}$ and where

$_{cn}$ are the chondrite normalised values using the CI concentrations reported by Anders and Grevesse, 1989) with trivalent REE at $\times 2_{cn}$ to $\times 24_{cn}$ (Fig. 3).

Elongate pyroxene crystals, which contribute to ~17 % by area of the clast, are associated with olivine and plagioclase grain boundaries and cross-cut the mesostasis. These have augite compositions (Fig. 4: En_{45-55} Fs_{8-12} Wo_{36-45}; Mg# = 79-86; Table EA S4). Minor element concentrations in pyroxene are plotted in Figure 5 and show that the clast has notably higher Al, Na, Ti, and marginally higher Cr concentrations (2.5-5 wt% Al_2O_3, 0.19-0.32 wt% Na_2O, 1.96-2.97 wt% TiO_2: Fig. 5) compared with similar Mg-rich lunar pyroxene (i.e., those from the Mg-Suite and KREEP basalts: Papike et al., 1998; Shervais and McGee, 1998; Taylor et al., 2012).

Fe/Mn ratios in olivine (46±10; quoted error is two standard deviations) and pyroxene (23±5) in the clast are significantly lower than Fe/Mn ratios in olivine (95±15) and pyroxene (57±13) in the host MAC 88105,159 meteorite (Figs. 8 and 9). They are also dissimilar in terms of Fe/Mn ratio to olivine and pyroxene in other lunar meteorites and Apollo samples (Figs. 6d, 8 and 9).

The remaining 11 % of the clast is composed of a K-rich, partially devitrified, interstitial glassy mesostasis with a bulk alkali-calcic dacite composition (Table 1). Also present in the clast are small (<10 µm) accessory (~0.5 %) Ti-rich phases (Fig. 2). Attempts to determine their nature was hampered by their small phase size, resulting in mixed analyses with surrounding minerals. The element maps of the clast reveal that two grains are Cr-bearing suggesting that at least two of the grains are probably Cr-bearing spinel. All the other grains are only Ti-bearing. In two cases the ratio of TiO_2/FeO measured in mixed EMPA analyses is more similar to ilmenite than Ti-rich spinel suggesting, thus, that some these grains are small ilmenite crystals, but this cannot be confirmed with the existing data. A mixed area of mesostasis

with some pyroxene and Ti-rich phases (see Fig. 2a where the left hand blue circle is located) has bulk trace elements with a negative Eu-anomaly (Eu/Eu* = 0.35) and trivalent REE of $\times 51_{cn}$ to $\times 133_{cn}$ (Fig. 3a, Table 1).

3.2 Clast Reconstructed Bulk Composition

The bulk composition of the clast is listed in Table 1. Major element composition was estimated by two independent approaches: (i) normalised raster-beam EDS analysis, where EDS X-ray spectra were collected from each digitised pixel of a selected region (polygon) of the clast. The accumulated X-ray counts were added together and in-built system matrix corrections performed on the total counts to derive element atomic abundances (see method of Joy et al., 2010a for full details), and (ii) modal recombination of the plagioclase (41 % by area), olivine (30% by area) and bulk mesostasis region (29% by area) compositions as listed in Table 1. The bulk trace element composition was estimated using the same modal recombination approach using the phase proportions listed above, and the mineral compositions listed in Table 1.

The modelled bulk clast composition supports the observations from mineral chemistry that the clast is both magnesian and rich in alkali (volatile) and incompatible elements (Table 1). (Table 1). In terms of bulk SiO_2 and alkalis it is classified as a basalt. It has essentially no Eu-anomaly (Eu/Eu* = 0.97, Fig. 3a) and, compared with bulk rock MAC 88104/05 (Joy et al., 2010a) it has high trivalent REE abundances (bulk MAC 88104/05: $\sim\times 6_{cn}$ to $\times 12_{cn}$; bulk clast: $\times 17_{cn}$ to $\times 51_{cn}$). It has K/Th ratios (~3000) that are an order of magnitude higher than the bulk lunar regolith observed from remote sensing measurements (the average lunar surface has a K/Th ratio of ~360: Peplowski et al., 2011, to ~810 in the northern farside

241 highlands: Gillis et al., 2004), but which are similar to some rare plutonic High Alkali Suite hand
242 specimen samples (as reported in the electronic index of Wieczorek et al., 2006).

243

244 3.3 Oxygen Isotope Results

245

246 In order to investigate whether or not the clast originated in the Earth-Moon system or elsewhere, we
247 performed *in situ* ion microprobe oxygen isotope analysis of plagioclase, olivine and pyroxene grains in
248 the clast and compared these data with oxygen isotopes measured in the host MAC 88105,159 lunar
249 material. The weighted mean of the host meteorite MAC 88105,159 lunar plagioclase grains (14 data
250 points) was assumed to lie on the terrestrial fractionation line (TFL) ($\Delta^{17}O = 0.00 \pm 0.15$, 2σ standard
251 error: Fig. 10 Table 2). The clast oxygen isotope data (8 data points) gave a weighted mean of $\Delta^{17}O =$
252 0.12 ± 0.20 (2σ standard error; Fig. 10). These results show in terms of $\Delta^{17}O$, the clast is statistically
253 indistinguishable from the TFL ($(0.12 \pm 0.20) - (0.00 \pm 0.15) = (0.12 \pm 0.25)$). Its weighted mean
254 composition is also statistically indistinguishable from the average of SNC (Shergottite-Nakhla-
255 Chassigny) martian meteorites (Fig. 10). However, the weighted mean of the clast is isotopically distinct
256 from the average composition of HED (Howardite-Eucrite-Diogenite) meteorites (Fig. 10) that are
257 thought to have originated from the asteroid Vesta.

258

259 **4. Discussion**

260

261 4.1. Petrological history. The mineral chemistry and bulk clast chemistry show that the clast is magnesian,
262 but also rich in alkali (volatile) and incompatible-trace elements. Although, we have to bear in mind that
263 the clast itself is very small, and may not be representative of its parent lithology (Warren, 2012), these
264 are unusual characteristics of a rock sourced from a primitive melt. It implies the presence of mixing of an
265 evolved melt component in the clast's parent melt source region or later assimilation of an evolved melt
266 component.

267

268 4.2 Origin. The clast has mineral-chemistry characteristics that differentiate it from known lunar
269 lithologies (Figs. 5, 6, 8 and 9). In particular the olivine and pyroxene crystals have Fe/Mn ratios that are
270 unique compared with previously sampled lunar rocks types. The ratio of Fe/Mn in mafic minerals and
271 bulk samples is indicative of planetary reservoirs and subsequent geological evolution of planetary bodies
272 (i.e., volatile loss, metal segregation during core removal, oxygen fugacity and melt fractionation: Drake
273 et al., 1989; Papike, 1998; Karner et al., 2003, 2006; Papike et al., 2003; Gross et al., 2011; Gross and
274 Treimen, 2010; Goodrich and Delaney, 2000). The possible planetary sources of the clast are discussed
275 below.

276

277 4.2.1 Sampling a unique region of lunar crust? Although the olivine and pyroxene mineral compositions
278 are not lunar-like (Figs. 5, 6 8 and 9), other characteristics maybe consistent with the clast being derived
279 from lunar rocks. Its magnesian nature is similar to rocks from the lunar Mg-Suite, although plagioclase is
280 alkali-rich compared to plagioclase in Mg-Suite rocks (Fig. 7). Conversely, although the clast's
281 aluminous and alkali-rich nature is more similar to samples from the High Alkali Suite, olivine and
282 pyroxene in the clast are too magnesian (Fig. 7). Plagioclase trace element concentrations (Fig. 3) are
283 similar to rocks from both the High Alkali Suite and Mg-Suite. If the rock is lunar, then it shares

284 characteristics of both these magmatic suites, although it differs from both. It is plausible that the rock
285 represents a Mg-Suite cumulate that was infiltrated by late stage evolved K-rich fluids (akin to High
286 Alkali Suite or KREEP basalt melts) to account for the alkali-rich plagioclase and trapped mesostasis Na-
287 K-rich glass.

288

289 If the clast originated from the Moon then an explanation is required for the non-lunar Fe/Mn ratios, in
290 both the early formed olivine (Figs. 8a and 8b) and the later crystallised pyroxene (Fig. 8c and 8d). The
291 following mechanisms could account for difference in Fe/Mn ratios between the clast and lunar rocks:

292

293 (1) Oxygen fugacity effects. Low Fe/Mn ratio in the clast could result from a source region with higher
294 fO_2 than typical lunar melts. However, no ferric mineral phases are present in the clast that would support
295 this model. Alternatively, the low ratio could imply that the clast has experienced reduction to remove Fe
296 from olivine and pyroxene, that could have decreased both mineral's Fe/Mg and Fe/Mn ratios, and
297 increased Ni concentrations in the clast compared with lunar rocks. However, no metallic Fe is observed
298 in the clast, so if reduction occurred, the resulting metal products and siderophile elements were
299 effectively removed from the rock before it crystallised.

300

301 (2) Crystallisation or fractionation effects. A decrease in Fe/Mn ratio in mafic phases could indicate that
302 olivine was removed (fractionated) from the sample's source region, as Mn is somewhat incompatible in
303 olivine and Fe is compatible (Humayun et al. 2004; Qin and Humayun, 2008); this process could decrease
304 the system's bulk Fe and increase the bulk Fe/Mg and decrease the Fe/Mn ratio. However, as the clast has
305 a bulk rock Mg# of 84-89 (Table 1), precipitating olivine in equilibrium should be Fo_{94-96} (calculated

using equation 3 of Joy et al., 2008 and references therein). As these calculated values are similar to the most primitive olivine composition measured in the clast (Fo_{93}), this indicates that little or no olivine was removed from the parent system and so this is not likely to be the cause of the Fe/Mn variation. Fe/Mn ratios could potentially also be lowered if Fe-Ti or Fe-Cr-Al oxides precipitated as an early phase removing Fe from the melt (Karner et al., 2003; Gross et al., 2011), however both olivine and pyroxene in the clast are generally Ti-rich, Cr-rich and Al-rich compared with lunar phases with similar Mg# (Figs. 5 and 6), suggesting that early oxide removal has not been extensive.

(3) Unique lunar crustal or mantle mineralogy. The lunar mantle and crust is heterogeneous, with regions that contain differing amounts of volatile elements (e.g., Hauri et al., 2011; McCubbin et al. 2011; Tartase et al., 2013). The clast could, therefore, have been sourced from a region with higher concentrations of volatile elements. Manganese is a moderately volatile element and generally has low concentrations in lunar materials, presumably because it was volatilised and depleted during the Moon's formation by giant impact (*e.g.*, Hartmann and Davis, 1975; Papike et al., 2003; O'Neill and Palme, 2008). However, in principle, as yet undiscovered relatively volatile-rich regions may exist in the lunar crust or mantle from which this clast might have been derived. An origin in such a region might also explain the relatively alkali-rich nature of the plagioclase grains within the clast.

In summary, although there are possibly mechanisms to account for the clasts's non-lunar-like Fe/Mn ratios in olivine and pyroxene, such models would also have to account for the clast's different mineral chemistry compared with known lunar rock types (Table 3). Indeed, the clast appears sufficiently compositionally unique compared with known lunar rocks that it may not be lunar at all.

329 4.2.2 A non-lunar origin? As the Fe/Mn ratios of the olivine and pyroxene are not lunar-like (Figs. 8 and
330 9), it is plausible that the clast may have been sourced from a different parent body and survived delivery
331 to the Moon as impact debris. Meteoritic debris have previously been identified on the Moon as rare
332 samples found in the lunar regolith (see Joy et al., 2012 for a summary).

333

334 Compositional and isotopic constraints for a meteoritic origin, and potential parent bodies, are listed in
335 Table 3. Olivine grains in the clast have non-lunar Fe/Mn ratios that are more similar to trends in martian
336 meteorites, terrestrial samples, and some chondrules in ordinary chondrites (Fig. 8). However, we do not
337 consider that the clast is a chondrule relic as there (i) are no Fe-metal, sulphide, Al-rich spinel or
338 nepheline grains present, indicative of plagioclase-rich chondrules; (ii) the clast bulk MgO/Al_2O_3 ratio
339 (~0.8) is lower than bulk chondrules (typically >>1.5: McSween, 1977), and clast bulk MgO/TiO_2 is
340 typically lower (<0.21) than in chondrules (typically >>45: McSween, 1977); and (iii) plagioclase grains
341 in the clast are a lot blockier than found in plagioclase-rich chondrules (Krot et al., 2002). The clast
342 pyroxenes have Fe/Mn ratios that are distinct from most basaltic achondrite groups, although are within
343 the spread of terrestrial pyroxene data (Fig. 8).

344

345 Additional constraints are provided by the oxygen isotope data. Minerals in the clast have oxygen-isotope
346 ratios (Table 2) that are (i) statistically indistinguishable from the Terrestrial Fractionation Line (*i.e.*., the
347 clast could be a terrestrial or a lunar sample); (ii) are statistically (2σ error) different from the bulk HED
348 meteorite trend; and (iii) are within 2σ error of the bulk SNC meteorite and angrite meteorite oxygen
349 isotope trends (Fig. 10).

350

Despite the fact that the oxygen isotopic composition is consistent with the TFL, and that the plagioclase An# values overlap with terrestrial values (Fig. 9), we provisionally discount a terrestrial origin for the clast. This is because the olivine Ni contents are lower (Clast = <150 ppm Ni: Table EA S1), than high-Fo ($Fo_{>80}$) olivine in terrestrial mafic rocks (typically >500 ppm Ni; Karner et al., 2003; PetDB database *www.**petdb**.org/*) and Archean samples (>600 ppm Ni; Barnes et al., 1983; Karner et al., 2003; Cheng and Kusky, 2007; Mondal et al., 2006; Pettigrew and Hattori, 2006). Additionally, although the Fe/Mn ratios in the clast's mafic phases overlap with examples from terrestrial samples, they do not exactly follow the terrestrial Fe/Mn ratio trend (Fig. 8).

It is notable that the Fe/Mn ratios in olivine fall very close to the martian olivine trend (Figs. 8a and 8b), and that the oxygen isotope values do not rule out a martian origin (Fig. 10). However, evidence from other mineral chemistry data appears to discount a martian source, as the olivine and pyroxene mineral compositions are atypically magnesian, and the plagioclase too Ca-rich (anorthitic) compared with known martian meteorites (*i.e.*, Papike et al., 2003, 2009; Karner et al., 2003; 2004; 2006; Sarbadhikari et al., 2011: Fig. 9). Moreover, unlike the olivine, the Fe/Mn ratios in pyroxene do not follow the martian trend (Karner et al., 2003; 2006; see Figs. 8 and 9). However, we have to recognise that our current set of martian meteorites are derived from a very few locations on Mars, and it would be unwise to assume that we have anything approaching a complete picture of the range of the composition of martian igneous rocks that we could use for such a comparison.

As we have no recognisable meteorite samples from Venus or Mercury to compare with, it is difficult to assess if these planets could have been the source of the clast. However, the clast bulk K (7300-8400 ppm; Table 1) and Th (~2.5 ppm) in the clast is notably higher than that recorded in any Mercury surface

374 regoliths by the Messenger mission gamma-ray spectrometer (GRS) instrument (1150 ± 220 ppm K; 0.22
375 ± 0.06 ppm Th; see Peplowski et al., 2011). It is also higher than that recorded by the GRS instrument on
376 board the Venera landers (3000-4500 ppm K; 0.7-2 ppm Th; see Fig. 2 of Peplowski et al., 2011 and
377 references therein). This suggests that the clast is unlike typical rocks in Mercury's or Venus's upper
378 crust, although clearly the full diversity of these crustal rocks is presumably greater than deduced from
379 relatively low spatial resolution orbital remote sensing of Mercury and three *in situ* measurements made
380 on Venus.

381

382 Compared with asteroid material sampled at the present day by near Earth objects (NEOs), mafic mineral
383 compositions in the clast are dissimilar to lithologies sampled by aubrite (Bearley and Jones, 1998),
384 winonaite (Benedix et al., 2005), acopulcoite, lodronite (McCoy et al., 1996, 1997), mesosiderite (Nehru
385 et al.1980) and ureilite (Downes et al., 2008) achondritic meteorites. Plagioclase grains in the clast are not
386 as calcic, and Fe/Mn ratios in olivine and pyroxene are lower than in angrite meteorites (Fig. 9, Papike et
387 al., 2003). Fe/Mn ratios and the augite-rich Na-bearing nature of pyroxene are also dissimilar to those in
388 HED pyroxene (Figs. 8c and 8d, and Fig. 9; see also McSween et al., 2012; Beck et al., 2012). HED
389 meteorites have already been shown to not fit well with the clast's oxygen-isotope composition (Fig. 10).

390

391 The clast could, therefore, have originated from a different, so-far unsampled, achondritic parent body
392 with differentiates that were melted from a primitive reserve (to account for magnesian mafic phases) and
393 included a fractionated residual liquid component (to account for the Na-K-rich mesostasis). Rare granitic
394 igneous fragments and glasses (some magnesian) have been reported in a number of meteorites that are
395 presumed to have originated within differentiated crusts by magmatism or impact processes on small
396 asteroidal parent bodies (e.g., Bonin, 2012). It is, therefore, possible that this clast could represent a

lithology from a differentiated asteroid parent body that is poorly represented, or not represented, in meteorites being delivered to Earth at the present day.

Whatever its source, *if* the clast is exogenous to the Moon, the timing of its delivery to the lunar surface could help to shed new light on the sources of projectiles being delivered to the Moon at different points in lunar history. Constraining the age of lunar regoliths is complicated as they contain many different rock types that may have undergone several formation and space-exposure episodes. In regolith samples that have undergone exposure to the space environment, the bulk-rock ratio of 'trapped' (parentless) ^{40}Ar to solar wind-implanted ^{36}Ar has been shown to be indicative of the last time the regolith system was closed from surface exposure (*i.e.,* it was turned from a soil into a rock). This isotope ratio can then be calibrated to a temporal antiquity age record using the argon isotope record of Apollo samples of known age (Eugster et al., 2001; Joy et al., 2011a). The trapped ^{40}Ar/^{36}Ar of MAC 88015 was measured by Eugster et al. (1991) to be 5.7. Applying this ratio to the age calibration of Joy et al. (2011a) implies that MAC 88105 was closed from lunar surface exposure at ~2.82 Ga. Therefore, any meteorite components in the MAC 88105 parent regolith would have to have been delivered to the lunar surface before this time. Eugster et al. (1991) report that the parent regolith was immature and had a surface residence time of about 650 Ma prior to brecciation: this implies that the clast possibly was delivered between ~3.47 Ga and ~2.82 Ga during Late Imbrian epoch to early Eratosthenian period.

Highly-siderophile-element signatures for impact melts (*e.g.,* Puchtel et al., 2008; Galenas et al., 2012; Fischer-Gödde and Becker, 2012), and discoveries of projectiles in ancient breccias (Joy et al., 2012), imply that chondritic asteroids were common sources of impactors during the basin-forming epoch (>3.7 Ga). Delivery of achondritic material to the lunar surface during an interval of ~3.47 Ga and ~2.82 Ga is

420 consistent with a variety of impactors (chondritic, achondritic, iron) found in younger Apollo 16 regolith
421 breccias and Apollo landing site soils (see Joy et al., 2012 for a summary), and reflects a possible
422 diversification of impactor sources in post-basin forming epoch (<3.7 Ga) projectile populations.

423

424 **4.3. Summary**

425

426 We have discovered a compositionally unusual clast within lunar meteorite MAC 88105,159. The clast is
427 composed of forsteritic olivine, bytownitic plagioclase, augitic pyroxene, and a mesostasis of devitrified
428 K-rich glass with an alkali-calcic dacite composition. In terms of olivine and pyroxene mineral Mg# it is
429 similar to Mg-Suite samples, however, in terms of An# plagioclase are sodic and more akin to samples of
430 the high alkali suite. This indicates that the rock may represent a new type of lunar lithology that
431 experienced an unusual petrological origin combining a primitive mafic melt with a late-stage alkali-
432 element (ITE-rich) component. However, despite these similarities to some known lunar rock types,
433 pyroxene and olivine in the clast have Fe/Mn ratios that are notably different from any known indigenous
434 lunar samples (Figs. 8 and 9). As Fe/Mn ratios are key indicators of planetary heritage, this evidence
435 suggests that the clast may not have originated from the Moon, and instead may represent material from
436 another differentiated parent body. We suggest that these Fe/Mn ratios and other unique compositional
437 characteristics point towards derivation from an achondritic basaltic meteorite that was derived from
438 parent body that was more oxidised and more volatile-rich, than the Moon.

439

440 Although in this study we have not been able to definitively identify the parent body from which this clast
441 is derived, the plausible discovery of an achondritic meteorite implanted in the lunar regolith prior to

442 ~2.82 Ga adds to the diverse suit of meteoritic material already known to be sampled in regolith breccias
443 and Apollo soils (see Joy et al., 2012 for a summary). This further underlines the importance of the lunar
444 regolith as an archive of impact debris derived from other bodies in the Solar System, including possible
445 samples of the early Earth of astrobiological significance that may not be preserved anywhere else (*e.g.*,
446 Armstrong et al., 2002; Crawford et al., 2008). Identifying such materials, both within the existing lunar
447 sample collection, and in samples collected by future lunar missions, will be an important aspect of lunar
448 science in the coming decades.

449

450 **Acknowledgements.** Thank you to Anne Peslier at JSC, John Spratt and Anton Kearsley at the NHM and
451 Andy Beard at Birkbeck for analytical assistance. We thank the referees Drs. Tomoko Arai, Duck
452 Mittlefehldt, James Karner and Juliane Gross, and AE Dr. Cyrena Goodrich for constructive comments.
453 This research was facilitated by Leverhulme Trust grants F/07 112/P to IAC and 2011-569 to KHJ. We
454 acknowledge a NASA Lunar Science Institute contract NNA09DB33A to David A. Kring PI which
455 supported the JSC EMP analyses and, grant NNX08AG58G to Gary R. Huss.

456

457 **References**

458

459 Armstrong J. C., Wells L. E., and Gonzales G. 2002. Rummaging through Earth's attic for remains of
460 ancient life. *Icarus* 160:183–196.

461

462 Anders E., and Grevesse N. 1989. Abundances of the elements: Meteoritic and solar *Geochimica et*
463 *Cosmochimica Acta* 53:197–214.

464

465 Beck A. W., Welten K. C., McSween H. Y. Jr., Viviano C. E., and Caffee M. W. (2012) Petrologic and
466 textural diversity among the PCA 02 howardite group, one of the largest pieces of the Vestan surface.
467 *Meteoritics & Planetary Science* 47: 947–969. doi: 10.1111/j.1945-5100.2012.01360.x

468

469 Barnes S.-J., Gorton M. P., and Naldrett A. J. 1983. A comparative study of olivine and clinopyroxene
470 spinifex flows from Alexo, abitibi greenstone Belt, Ontario, Canada. *Contributions to Mineralogy and*
471 *Petrology* 83:293–308. doil: 10.1007/BF00371198

472

473 Benedix G. K., Lauretta D. S., and McCoy T. J. 2005. Thermodynamic constraints on the formation
474 conditions of winonaites and silicate-bearing IAB irons**.** *Geochimica et Cosmochimica Acta* 69:5123–
475 5131.

476

477 Berlin J., Jones R. H., and Brearley A. J. 2011. Fe-Mn systematics of type IIA chondrules in
478 unequilibrated CO, CR, and ordinary chondrites. *Meteoritics & Planetary Science* 46:513–533. doi:
479 10.1111/j.1945-5100.2011.01171.x

480

481 Bonin B. 2012. Extra-terrestrial igneous granites and related rocks: A review of their occurrence and
482 petrogenesis. *Lithos* 153:3–24

Brearley A.J., and Jones R.H. 1998. Chondritic meteorites. In *Mineralogical Society of America Reviews in Mineralogy, Volume 36. Planetary Materials*. (Ed. J.J. Papike). 400 pp.

Cheng S., and Kusky T. 1997. Komatiites from west Shandong, North China craton: Implications for plume tectonics. *Gondwana Research* 12:77–83. doi.org/10.1016/j.gr.2006.10.015.

Cohen B. A., Swindle T. D., and Kring D. A. 2005. Geochemistry and ^{40}Ar-^{39}Ar geochronology of lunar highland meteorite impact melt clasts. *Meteoritics & Planetary Science* 40:755–777.

Crawford I. A., Baldwin E.C., Taylor E.A., Bailey J., and Tsembelis K., 2008. On the survivability and detectability of terrestrial meteorites on the Moon. *Astrobiology* 8:242–252.

Crawford I. A., Fagents S. A., Joy K. H., and Rumpf M. E. 2010. Lunar Palaeoregolith Deposits as Recorders of the Galactic Environment of the Solar System and Implications for Astrobiology. *Earth, Moon and Planets* 107:75–85. doi:10.1007/s11038-010-9358-z

Delano J.W. 1991. Geochemical comparison of impact glasses from lunar meteorites ALHA and MAC88105 and Apollo 16 regolith 64001. *Geochimica et Cosmochimica Acta* 55:3019–3029.

503 Downes H., Mittlefehldt, D.W., Kita N.T., and Valley J.W. 2008. Evidence from polymict ureilite
504 meteorites for a disrupted and re-accreted single ureilite parent asteroid gardened by several distinct
505 impactors. *Geochimica et Cosmochimica Acta* 72(19):4825–4844. doi: /10.1016/j.gca.2008.06.028

506

507 Eugster O., Burger M., Krähenbühl U., Michel Th., Beer J., Hofmann H. J., Synal H. A., Woelfli W., and
508 Finkel R. C. 1991. History of the paired lunar meteorites MAC 88104 and MAC 88105 derived from
509 noble gas isotopes, radionuclides, and some chemical abundances. *Geochimica et Cosmochimica Acta*
510 55:3139–3148.

511

512 Eugster O., Terribilini D., Polnau E., and Kramers J. 2001. The antiquity indicator argon-40/argon-36 for
513 lunar samples calibrated by uranium-235-xenon-136 dating. *Meteoritics & Planetary Science* 36:1097–
514 1115.

515

516 Fagan A. L., Neal C. R., Simonetti A. , Donohue P. H., and K. M. O'Sullivan. 2013. Distinguishing
517 between Apollo 14 impact melt and pristine mare basalt samples by geochemical and textural analyses of
518 olivine. *Geochimica et Cosmochimica Acta* 106:429–445.

519

520 Fischer-Gödde M., and Becker H. 2012. Osmium isotope and highly siderophile element constraints on
521 ages and nature of meteoritic components in ancient lunar impact rocks. *Geochimica et Cosmochimica*
522 *Acta* 77:135–156.

523

524 Floss C. A., James A. B., McGee J. J., and Crozaz G. 1998. Lunar ferroan anorthosite petrogenesis: Clues
525 from trace element distributions in FAN subgroups. *Geochimica et Cosmochimica Acta* 62: 1255–1283.

526

527 Fruland R.M. 1983. Regolith Breccia Workbook. Curatorial Branch Publication #66. JSC 19045.

528

529 Galenas M. G., Liu J. G., and Walker R. J. 2012. $^{187}Os/^{188}Os$ and Highly Siderophile Element
530 Characteristics of Apollo 16 and 17 Impact-melt Breccias. Workshop on Early Solar System Impact
531 Bombardment II (2012) (abstract #4003).

532 Gillis J. J., Jolliff B. L., and, Korotev R. L. 2004 Lunar surface geochemistry: Global concentrations of
533 Th, K, and FeO as derived from Lunar Prospector and Clementine data. *Geochimica et Cosmochimica*
534 *Acta* 68, 3791–3805

535

536 Goodrich C. A., and Delaney J. S. 2000. Fe/Mg–Fe/Mn relations of meteorites and primary heterogeneity
537 of primitive achondrite parent bodies. *Geochimica et Cosmochimica Acta* 64:149–160.

538

539 Gross J., and Treiman A.H. 2010. Dispersed Fe/Mn ratios of lunar rocks: ALH 81005's view from the
540 Farside. Goldschmidt 2010 (abstract #2557).

541

542 Gross J., Treiman A.H., and Filiberto J. 2011. Constraints on the geochemical variations and evolution of
543 the lunar crust and mantle as revealed by Fe, Mn, and Cr correlations in olivine. (abstract #2805). 42nd
544 Lunar and Planetary Science Conference.

545

546 Hartmann W.K., and Davis D.R., 1975. Satellite-sized planetesimals and lunar origin. *Icarus* 24:504–515.

547

548 Hauri E H., Weinreich T., Saal A. E., Rutherford M. C., and Van Orman J. A. 2011. High Pre-Eruptive
549 Water Contents Preserved in Lunar Melt Inclusions. *Science* 333:213-215. DOI: 10.1126/science.1204626

550

551 Hörz F., Grieve R., Heiken G., Spudis P., and Binder A. 1991. Lunar surface processes. In Lunar
552 Sourcebook – A Users Guide to the Moon, edited by Heiken G., Vaniman D., and French B.Cambridge
553 University Press. pp. 1–120.

554

555 Humayun M., Qin L. and Norman M. D. 2004. Geochemical evidence for excess iron in the mantle
556 beneath Hawaii. *Science* 306:91–94.

557

558 Ikeda Y., and Takeda H. 1985. A model for the origin of basaltic achondrites based on the Yamato 7308
559 Howardite *Journal of Geophysical Research: Solid Earth* *90*(S02):C649–C663. doi:
560 10.1029/JB090iS02p0C649.

561

562 Jolliff B.L., Korotev R.L., and Haskin L.A. 1991. A ferroan region of the lunar highlands as recorded in
563 meteorites MAC88104 and MAC88105. *Geochimica et Cosmochimica Acta* 55:3051–3071.

564

565 Jolliff B.L., Floss C., McCallum I.S., and Schwartz J.M. 1999. Geochemistry, petrology, and cooling
566 history of 14161,7373: A plutonic lunar sample with textural evidence of granitic-fraction separation by
567 silicate-liquid immiscibility. *American Mineralogist* 84:821–837.

568

569 Joy K. H., Crawford I. A., Downes H., Russell S. S., and Kearsley A. T. 2006. A Petrological,
570 Mineralogical and Chemical Analysis of the Lunar Mare Basalt Meteorites LaPaz Icefield 02205, 02224
571 and 02226. *Meteoritics and Planetary Science* 41:1003-1026.

572

573 Joy K. H., Crawford I. A., Anand M., Greenwood R.C., Franchi I.A. and Russell S. S. 2008. The
574 Petrogenesis of Miller Range 05035: A New Lunar Gabbroic Meteorite. *Geochimica et Cosmochimica*
575 *Acta* 72:3822–3844.

576

577 Joy K. H., Crawford I.A., Russell S. S., and Kearsley A. T. 2010a. Lunar Meteorite Regolith Breccias: an
578 *in situ* study of impact melt composition using LA-ICP-MS and implications for the composition of the
579 lunar crust. *Meteoritics & Planetary Science* 45:917–946.

580

581 Joy K. H., Crawford I. A. and Snape J. F. 2010b. Lunar Meteorite Miller Range 07006: Petrography and
582 VLT Basalt Clast Inventory (abstract #1793), 41st Lunar and Planetary Science Conference, Houston.

Joy K.H., Kring D.A., Bogard D.D., McKay D.S., and Zolensky M.E. 2011a. Re-examination of the formation ages of the Apollo 16 regolith breccias. *Geochimica et Cosmochimica Acta* 75:7208–7225.

Joy K. H., Ross D. K., Zolensky M. E., and Kring D. A. 2011b. Reconnaissance Element Mapping of Lunar Regolith Breccias. 2011 Annual Meeting of the Lunar Exploration Analysis Group (abstract #2007)

Joy K. H., Burgess R., Hinton R., Fernandes V. A., Crawford I. A., Kearsley A. T., Irving A. J., and EIMF 2011c. Petrogenesis and Chronology of Lunar Meteorite Northwest Africa 4472. *Geochimica et Cosmochimica Acta.* 75:2420-2452. doi:10.1016/j.gca.2011.02.018.

Joy K. H., Zolensky M. E., Nagashima K., Huss G.R., Ross D. K., McKay D. S., and Kring D. A., 2012. Direct detection of projectile relics from the end of the lunar basin–forming epoch. *Science* 336: 1426–1429.

Karner J., Papike J.J ., and Shearer C. K. 2003. Olivine from planetary basalts: Chemical signatures that indicate planetary parentage and those that record igneous setting and process. *American Mineralogist* 88:806–816.

602 Karner J., Papike J. J., and Shearer C.K. 2004. Plagioclase from planetary basalts: Chemical signatures
603 that reflect planetary volatile budgets, oxygen fugacity, and styles of igneous differentiation *American*
604 *Mineralogist* 89:1101–1109.

605

606 Karner J., Papike J. J., and Shearer C. K. 2006. Comparative planetary mineralogy: Pyroxene major- and
607 minor-element chemistry and partitioning of vanadium between pyroxene and melt in planetary basalts
608 *American Mineralogist* 91:1574–1582, doi: 10.2138/am.2006.2103 1574.

609

610 Koeberl C., Kurat G., and Brandstätter F. 1991. MAC88105-A regolith breccia from the lunar highlands:
611 mineralogical, petrological, and geochemical studies. *Geochimica et Cosmochimica Acta* 55:3073–3087.

612

613 Korotev R.L., Jolliff B. L., Zeigler R. A., Gillis J. J., and Haskin L. A. 2003. Feldspathic lunar meteorites
614 and their implications for compositional remote sensing of the lunar surface and the composition of the
615 lunar crust. *Geochimica et Cosmochimica Acta* 67:4895–4923.

616

617 Krot A. N., Hutcheon I. D., and Keil K. 2002. Plagioclase-rich chondrules in the reduced CV chondrites:
618 Evidence for complex formation history and genetic links between calcium-aluminum-rich inclusions and
619 ferromagnesian chondrules *Meteoritics* & *Planetary Science* 37:155-182.

620

621 Lindstrom M. M., Wentworth S. J., Martinez R. R., Mittlefehldt D. W., McKay D. S., Wang M.-S., and
622 Lipschutz M. J. 1991. Geochemistry and petrography of the MacAlpine Hills lunar meteorites.
623 *Geochimica et Cosmochimica Acta* 55:3089–3103.

624

625 Lucey P., Korotev R. L., Gillis J. J., Taylor L. A., Lawrence D., Campbell B. A., Elphic R., Feldmann B.,
626 Hood L.L., Hunten D., Mendillo M., Noble S., Papike J. J., Reedy R. C., Lawson S., Prettyman T.,
627 Gasault O., and Maurice S. 2006. Understanding the Lunar Surface and Space-Moon Interactions. In New
628 Views of the Moon, *edited by* Jolliff B. L., Wieczorek M. A., Shearer C. K., and Neal C. R. *Rev. Mineral.*
629 *Geochem* 60:83–219.

630

631 Makide K., Nagashima K., Krot A.N., Huss G.R., Hutcheon I.D., and Bischoff A. 2009. Oxygen- and
632 magnesium-isotope compositions of calcium-aluminum-rich inclusions from CR2 carbonaceous
633 chondrites. *Geochimica et Cosmochimica Acta* 73:5018-5050.

634

635 McCoy T.J., Keil K., Clayton R. N., Mayeda T. K., Bogard D. D., Garrison D. H., Huss G. R., Hutcheon
636 I. D., and Wieler R. 1996. A petrologic, chemical and isotopic study of Monument Draw and comparison
637 with other acapulcoites: Evidence for formation by incipient partial melting. *Geochimica et*
638 *Cosmochimica Acta* 60:2681–2708.

639

McCoy T. J., Keil K., Clayton R. N., Mayeda T. K., Bogard D. D., Garrison D. H., and Wieler R. 1997. A petrologic and isotopic study of lodranites: Evidence for early formation as partial melt residues from heterogeneous precursors. *Geochimica et Cosmochimica Acta* 61:623–637.

McCubbin F. M., Jolliff B. L., Nekvasil H., Carpenter P. K., Zeigler R. A., Steele A., Elardo S. M., and Lindsley D. H. Fluorine and chlorine abundances in lunar apatite: Implications for heterogeneous distributions of magmatic volatiles in the lunar interior. *Geochimica et Cosmochimica Acta* 75:5073-5093

McKay D. S., Bogard D. D, Morris R. V., Korotev R. L., Johnson P., and Wentworth S. J. 1986. Apollo 16 Regolith Breccias: Characterization and Evidence for Early Formation in the Mega-Regolith. In *Lunar and Planetary Science XVI* in *Journal of Geophys. Res.* 91:D277–D303.

McKay D. S., Heiken G., Basu A., Blanford G., Simon S., Reedy R., French B. M., and Papike J. 1991. The Lunar Regolith. InLunar Sourcebook – A Users Guide to the Moon, edited by Heiken G., Vaniman D., and French B.Cambridge University Press. . pp. 285-356.

McSween H. Y. Jr., Mittlefehldt D. W., Beck A.W., Mayne R. G., and McCoy T. J. 2012. HED Meteorites and Their Relationship to the Geology of Vesta and the Dawn Mission *Space Sci. Rev.* doi.I 10.1007/s11214-010-9637-z.

660 McSween H. Y. Jr. 1977. Chemical and petrographic constraints on the origin of chondrules and
661 inclusions in carbonaceous chondrites. *Geochimica et Cosmochimica Acta* 41:1843

662

663 Mittlefehldt D. W. Clayton R. N., Drake M. J., Righter K. 2008. Oxygen Isotopic Composition and
664 Chemical Correlations in Meteorites and the Terrestrial Planets. *In* Oxygen in the solar system. *Reviews*
665 *in Mineralogy and Geochemistry* 68:399-428

666

667 Mondal S. K., Ripley E. M., Li C., and Frei R. 2006. The genesis of Archaean chromitites from the
668 Nuasahi and Sukinda massifs in the Singhbhum Craton, India. *Precambrian Research* 148:45–66.

669

670 Neal C.R., Taylor L.A., Liu Y., and Schmitt R.A. 1991. Paired lunar meteorites MAC88104 and
671 MAC88105: a new "FAN" of lunar petrology. *Geochimica et Cosmochimica Acta* 55:3037–3049.

672

673 Nehru C.E., Zucker S.M., Harlow G.E., and Prinz M. 1980. Olivines and olivine coronas in mesosiderites.
674 *Geochimica et Cosmochimica Acta* 44:1103–1118.

675

676 O'Neill H. St. C., and Palme H. 2008. Collisional erosion and the non-chondritic composition of the
677 terrestrial planets. *Phil. Trans. R. Soc. A* 366:4205–4238. doi:10.1098/rsta.2008.0111.

678

679 Papike J. J. 1998. Comparative planetary mineralogy; chemistry of melt-derived pyroxene, feldspar, and
680 olivine. In *Mineralogical Society of America Reviews in Mineralogy, Volume 36. Planetary Materials*.
681 (Ed. J.J. Papike). pp. 7.1-7.11

682

683 Papike J. J., Taylor L., and Simon S. 1991. Lunar Minerals. In *Lunar sourcebook: A user's guide to the*
684 *moon*: Edited by Grant H. Heiken David Vaniman and Bevan M. French. Cambridge University Press,
685 1991. (ISBN 0-521-33444-6).

686

687 Papike J. J., Fowler G. W., Shearer C. K. and Layne G. D. 1996. Ion microprobe investigation of
688 plagioclase and orthopyroxene from lunar Mg-suite norites: implications for calculating parental melt
689 REE concentrations and for assessing postcrystallization REE redistribution. *Geochimica et*
690 *Cosmochimica Acta* 60:3967–3978.

691

692 Papike J. J., Fowler G. W., and Shearer C. K. 1997. Evolution of the lunar crust: SIMS study of
693 plagioclase from ferroan anorthosites. *Geochimica et Cosmochimica Acta* 61:2343–2350.

694

695 Papike J. J., Ryder G., and Shearer C.K. 1998. Lunar Samples. In *Mineralogical Society of America*
696 *Reviews in Mineralogy, Volume 36. Planetary Materials*. (Ed. J.J. Papike). 400 pp..

697

698 Papike J.J., Karner J.M, and Shearer C.K. 2003. Determination of planetary basalt parentage: A simple
699 technique using the electron microprobe. *American Mineralogist* 88:469–472.

Papike J.J., Karner J.M, Shearer C.K. and Burger P. V. 2009. Silicate mineralogy of martian meteorites *Geochimica et Cosmochimica Acta* 73:7443–7485.

Pearce N. J. G., Perkins W. T., Westgate J. A., Gorton M. P., Jackson S. E., Neal C. R., and Chenery S. P. 1997. New data for the National Institute of Standards and Technology 610 and 612 glass reference materials. *Geostandards Newsletter* 21:115–144.

Peplowski P. N., Evans L. G., Hauck S. A. II, McCoy T. J., Boynton W. V., Gillis-Davis J. J., Ebel D. S., Goldsten J. O., Hamara D. K., Lawrence D. J., McNutt Jr.R. L.,1 Nittler L.R., Solomon S. C., Rhodes E. A., Sprague A. L., Starr R. D., and Stockstill-Cahill K. R. 2011. Radioactive Elements on Mercury's Surface from MESSENGER: Implications for the Planet's Formation and Evolution. *Science* 333:1850–1852. doi: 10.1126/science.1211576.

Pettigrew N.T., and Hattori K. H. 2006. The Quetico Intrusions of Western Superior Province: Neo-Archean examples of Alaskan/Ural-type mafic–ultramafic intrusions. *Precambrian Research* 149:21–42.

Puchtel I. S., Walker R. J., James O. B., and Kring D. A. 2008. Osmium isotope and highly siderophile element systematics of lunar impact melt breccias: Implications for the late accretion history of the Moon and Earth. *Geochimica et Cosmochimica Acta* 72(12):3022–3042

721 Qin L., and Humayun M. 2008. The Fe/Mn ratio in MORB and OIB determined by ICP-MS. *Geochimica*
722 *et Cosmochimica Acta* 72:1660–1677. doi.org/10.1016/j.gca.2008.01.012

723

724 Robinson K. L., Treiman A.H., and Joy K. H. 2012. Basaltic fragments in lunar highlands meteorites:
725 connecting sample analyses to orbital remote sensing. *Meteoritics & Planetary Science* 47:387–399. doi:
726 10.1111/j.1945-5100.2012.01344.x.

727

728 Rumble D., Irving, A. J., Bunch T. E., Wittke J. H., Kuehner S. M. 2008. Oxygen Isotopic and
729 Petrological Diversity Among Brachinites NWA 4872, NWA 4874, NWA 4882 and NWA 4969: How
730 Many Ancient Parent Bodies? *Lunar and Planetary Science XXXIX*, Abstract #1974.

731

732 Sarbadhikari A. B., Goodrich C. A., Liu Y., Day J. M. D., and Taylor L. A. 2009. Evidence for multiple
733 enriched shergottite mantle sources in Mars from olivine-hosted melt inclusions in Larkman Nunatak
734 06319. *Geochimica et Cosmochimica Acta* 75:6803–6820.

735

736 Schnare D.W., Day J.M.D., Norman M.D., Liu Y., and Taylor L.A. 2008. A laser-ablation ICP-MS study
737 of Apollo 15 low-titanium olivine-normative and quartz-normative mare basalts. *Geochimica et*
738 *Cosmochimica Acta* 72:2556–2572.

739

740 Shearer C. K., and Papike J. J. 2005. Early crustal building processes on the moon: models for the
741 petrogenesis of the magnesian suite. *Geochimica et Cosmochimica Acta* 69:3445–3461.

Shervais J. W., and McGee J. J. 1998. Ion and electron microprobe study of troctolites, norite, and anorthosites from Apollo 14: Evidence for urKREEP assimilation during petrogenesis of Apollo 14 Mg-suite rocks. *Geochimica et Cosmochimica Acta* 62(17): 3009–3023.Shervais J. W., and McGee J. J. 1999. KREEP cumulates in the western lunar highlands: Ion and electron microprobe study of alkali-suite anorthosites and norites from Apollo 12 and 14. *American Mineralogist* 84:806–820.

Snape J. F., Beaumont S., Burgess R., Crawford I. A., Joy K. H. 2011. An evaluation of techniques used in the age and petrologic analysis of Apollo 12 basalts. *Lunar and Planetary Science XLII*, Abstract #2011.

Tartèse R., Anand M., Barnes J. J., Starkey N.A., Franchi, I. A., and Sano Y. 2013. The abundance, distribution, and isotopic composition of Hydrogen in the Moon as revealed by basaltic lunar samples: implications for the volatile inventory of the Moon. *Geochimica et Cosmochimica Acta.* 122:58-74. Doi: http://dx.doi.org/10.1016/j.gca.2013.08.014.

Taylor G. J. 1991. Impact melts in the MAC88105 lunar meteorite: nferences for the lunar magma ocean hypothesis and the diversity of basaltic impact melts. *Geochimica et Cosmochimica Acta* 55:3031–3036.

Taylor G. J., Martel L. M. V., and Spudis P. D. 2012. The Hadley-Apennine KREEP basalt igneous province *Meteoritics & Planetary Science* 47:861–879. doi: 10.1111/j.1945-5100.2012.01364.x

763 Takeda H., Miyamoto M., Ishii T., and Lofgren G.E. 1975. Relative cooling rates of mare basalts at the
764 Apollo 12 and 15 sites as estimated from pyroxene exsolution data. Proceedings, 6th Lunar Science
765 Conference. pp. 987–996.

766

767 Takeda H., Mori H., Ikeda Y., Teruaki I., and Yanai K. 1984. Antarctic howardites and their primitive
768 crust. *Mem. Natl. Inst. Polar Res., Spec. Issue* 31:81–101.

769

770 Warren P. H. 1989. KREEP: major-element diversity, trace element uniformity (Almost) Workshop on
771 Moon in transition: Apollo 14, KREEP, and evolved lunar rocks. In LPI Technical Report 89-03, edited
772 by G. J. Taylor and P. H. Warren. Lunar and Planetary Institute. p. 149.

773

774 Warren P. H. 1993. A concise compilation of petrologic information on possibly pristine non mare Moon
775 rocks *American Mineralogist* 78:360–376.

776

777 Warren P. H. 2012. Let's get real: not every lunar rock sample is big enough to be representative for
778 every purpose. *Second Conference on the Lunar Highlands Crust (2012)* Abstr. #9034.

779

780 Warren P. H., and Kallemeyn G. W. 1991. The MacAlpine Hills lunar meteorite and implications of the
781 lunar meteorites collectively for the composition and origin of the Moon. *Geochimica et Cosmochimica*
782 *Acta* 55:3123–3138.

Wieczorek M. A., Jolliff B. L., Khan A., Pritchard M. E., Weiss B. P., Williams J. G., Hood L. L., Righter K., Neal C. R., Shearer C. K., McCallum I. S., Tompkins S., Hawke B. R., Peterson C., Gillis J. J., and Bussey B. 2006. The constitution and structure of the lunar interior. In *New Views of the Moon*, *Rev. Mineral. Geochem*. 60:221–364.

Wieler R. 1998. The Solar Noble Gas Record in Lunar Samples and Meteorites. *Space Science Reviews* 85(1-2):303–314, doi: 10.1023/A:1005166904225

Table captions

Table 1. Major (EMPA) and trace element (LA-ICP-MS) composition of an olivine grain, a plagioclase grain and a mixed mesostasis area (pyroxene and K-rich glass and Ti-phases) in the clast in MAC 88105,159. Also listed is the bulk composition of the clast estimated (i) by a raster-beam EDS analysis (see Joy et al., 2010a for details) and (ii) by modal reconstruction using proportions 30% plagioclase, 28 olivine and 30% mesostasis (Fig. 1).

Table 2. Results of *in situ* oxygen isotope studies. Data were collected from plagioclase in host meteorite MAC 88105,159 (top) and minerals phases in the clast (bottom). The weighted mean $\Delta^{17}O$ of the lunar plagioclase was normalised to the TFL ($\Delta 17O = 0$) and then the lunar dataset and clast dataset were normalised by the same amount (right hand columns). Weighted mean host MAC 88105,159 data and

clast data errors are 2σ standard error (standard deviation of data divided by the square root of number of measurements).

Table 3. Summary of compositional and mineralogical similarities and differences between the clast in MAC 88105,159 and other planetary bodies.

Figure Captions

Figure 1. (a) Back-scatter electron image and (b) false-colour element maps of sample MAC 88105,159. For the false-colour map image pixels are coloured to denote distribution and concentration of magnesium (green), aluminium (white), iron (red), silica (blue), titanium (pink), calcium (yellow) and potassium (cyan) (after Joy et al., 2011b). Location of the clast, which appears green as it is magnesian, is indicated with a red square inlay. Other green phases in the sample are olivine-rich clasts or single olivine mineral fragments.

Figure 2. Close up images of clast in MAC 88105,159. (a) Back-scatter electron image of clast. Red circles denote collection locations and size of SIMS oxygen measurements. Blue circles denote location and size of LA-ICP-MS pits for trace element analysis. (b) False colour element map of the clast (see figure 1b for colour details). Minerals phases are denoted where Ol = olivine, pyx = pyroxene, plag = plagioclase and ms = mesostasis. (c) Mineral distribution within the clast where blue = plagioclase, red =

824 olivine, green = pyroxene, yellow = mesostasis glass, pink = Ti-rich phase and white = holes or host
825 meteorite MAC 88105,159.

826

827 Figure 3. REE concentrations in the clast (Table 1). (a) CI chondrite-normalised REE values of
828 plagioclase and olivine mineral grains and bulk area mesostasis (glass + ilmenite + pyroxene). REE
829 abundances of CI chondrite were from Anders and Grevesse (1989). Also shown are the modelled (modal
830 recombination) bulk clast composition (Table 1) and the composition of high-K KREEP (Warren, 1989)
831 for comparison. (b) Clast plagioclase REE value compared with those from the lunar ferroan anorthosite
832 (FAN) suite (Papike et al., 1997; Floss et al., 1998), the Mg-Suite (HMS: medium grey box: data from
833 Papike et al., 1996; Shervais and McGee, 1998) and the High Alkali Suite (HAS: dark grey box: data
834 from Shervais and McGee, 1999). Error bars shown are 2 sigma.

835

836 Figure 4. Pyroxene compositions measured in the clast plotted onto a pyroxene quadrilateral. Data are
837 compared with pyroxene in clasts and mineral fragments in the host MAC 88105,159 meteorite and also
838 in MAC 88104,47, MAC 88105,158 and MAC 88104,48.

839

840 Figure 5. Minor elements in pyroxene in the clast compared with pyroxene in lunar meteorites and Apollo
841 samples. Note that for a given Mg# the clast pyroxene have higher concentrations of Na, Ti, and Al
842 compared to most other lunar materials. Meteoritic data sources are as follows: MAC 88104/05, Dar al
843 Gani 400, Meteorite Hills 01210 and Pecora Escarpment 02007: Joy et al. (2010a); North West Africa
844 4472: Joy et al. (2011c); Miller Range 07006: Joy et al. (2010b); Robinson et al. (2012); La Paz 02205
845 and pairs Joy et al. (2006); and Miller Range 05035: Joy et al. (2008). Data for Apollo samples, includes

feldspathic lithologies, Mg-Suite, KREEP and mare basalts (Takeda et al., 1975; Papike et al., 1991; 1996; 1998; Shervais and McGee, 1999; Jolliff et al., 1999; Schnare et al., 2008; Taylor et al., 2012).

Figure 6. Minor elements in olivine in the clast compared with olivine in lunar meteorites (see Fig. 5 caption for literature sources) and Apollo samples including feldspathic lithologies, Mg-Suite, KREEP and mare basalts (see Fig. 5 caption for literature sources). Note that for a given Mg# the clast olivine have equivalent Ca and Ti higher concentrations of Cr and lower FeO/MnO ratios.

Figure 7. Average Mg# of olivine and pyroxene vs. plagioclase 100×Ca/[Ca+Na] (average 79) in the clast. Error bars show range of compositions in the clast. Note that the clast plagioclase data has been recalculated from that presented in the text which was reported for 100×Ca/[Ca+Na+K]. The data are compared with possibly pristine non-mare rocks listed by Warren (1993). The outer ferroan anorthosite suite (FAS) field was taken from Warren (1993). The inner ferroan anorthosite suite field and High Mg-Suite (HMS) fields outline those rocks that have high confidence of pristinity (i.e., those with pristinity values of >8: Warren, 1993). The approximate boundary (dashed line) between Mg-Suite and High Alkali Suite rocks was taken from Wieczorek et al. (2006).

Figure 8. Mn vs. total Fe atoms per formula unit in (a) and (b) olivine, and (c) and (d) pyroxene in the clast. Data in in (a) and (c) are compared with mafic phases in other lunar meteorites and numerous Earth rocks (taken from the PetDB database including basalts, peridotites, lherzolite, troctolites, gabbros, gabbronorite, harzbergites etc. where reported Fe data is converted from wt% FeO_{total}). Also shown are average planetary trend lines where the Moon lines are linear fits (olivine: Mn = [0.0114×Fe]-0.0003;

pyroxene: Mn = [0.0116×Fe]-0.0038) to lunar meteorite pyroxene and olivine data as reported in Fig. 5 caption; the Earth line is taken from a linear fit (olivine: Mn = [0.0194×Fe]-0.0015; pyroxene: Mn = [0.0309×Fe]-0.0028) to data compiled in the PetDB database from numerous terrestrial rocks; planetary trend lines for SNC meteorites (Mars) and HED meteorites (Vesta) are from Papike et al. (2009), and ordinary chondrites (OC) and CO-type carbonaceous chondrites are from Berlin et al. (2011). In (b) and (d) data from olivine and pyroxene phases in lunar meteorite MAC 88104/05 (Joy et al., 2010a and this study), and Apollo Mg-Suite is plotted for comparison (Papike et al., 1998; Shervais and McGee, 1998).

Figure 9. Range of typical plagioclase composition (where An# = Ca/[Ca+Na+K]) vs. olivine and pyroxene atomic Mn/Fe ratios for different planetary bodies (fields for meteorite groups, Earth and Apollo basalts taken from Papike et al., 2003). Also shown are the total range of plagioclase, pyroxene and olivine compositions reported in lunar meteorites (references listed in Fig. 5 caption. Average composition of the MAC 88105,159 clast is plotted in red where the bars denote the range in composition plagioclase and mafic phases.

Figure 10. Time order analysis of $\Delta^{17}O$ oxygen isotope analysis of phases in the lunar portion of host meteorite MAC 88105,159 (grey symbols) where the weighted mean (grey line and square grey symbol) has been normalised to the TFL. $\Delta^{17}O$. The 2σ standard errors of these lunar measurements (± 0.15) is shown as error bars on grey square symbol. Analyses of phases in the clast are shown as red symbols where the weighted mean (normalised to the weighted mean of the lunar portion corrected to the TFL) is $\Delta^{17}O = 0.12$ shown as the solid red line and red square symbol. The 2σ uncertainty (± 0.25) levels for the mean of the clast (including the standard error on the means for both the clast and lunar measurements) are shown as error bars on the red square symbol. These errors are appropriate to compare the $\Delta^{17}O$ of the

clast with those of average SNC ($\Delta^{17}O$ 0.29: average of data compiled by Mittlefehldt et al., 2008), HED ($\Delta^{17}O$ -0.22: average of data compiled by Mittlefehldt et al., 2008) and angrite meteorites ($\Delta^{17}O$ -0.07: Rumble et al., 2008).

Figures

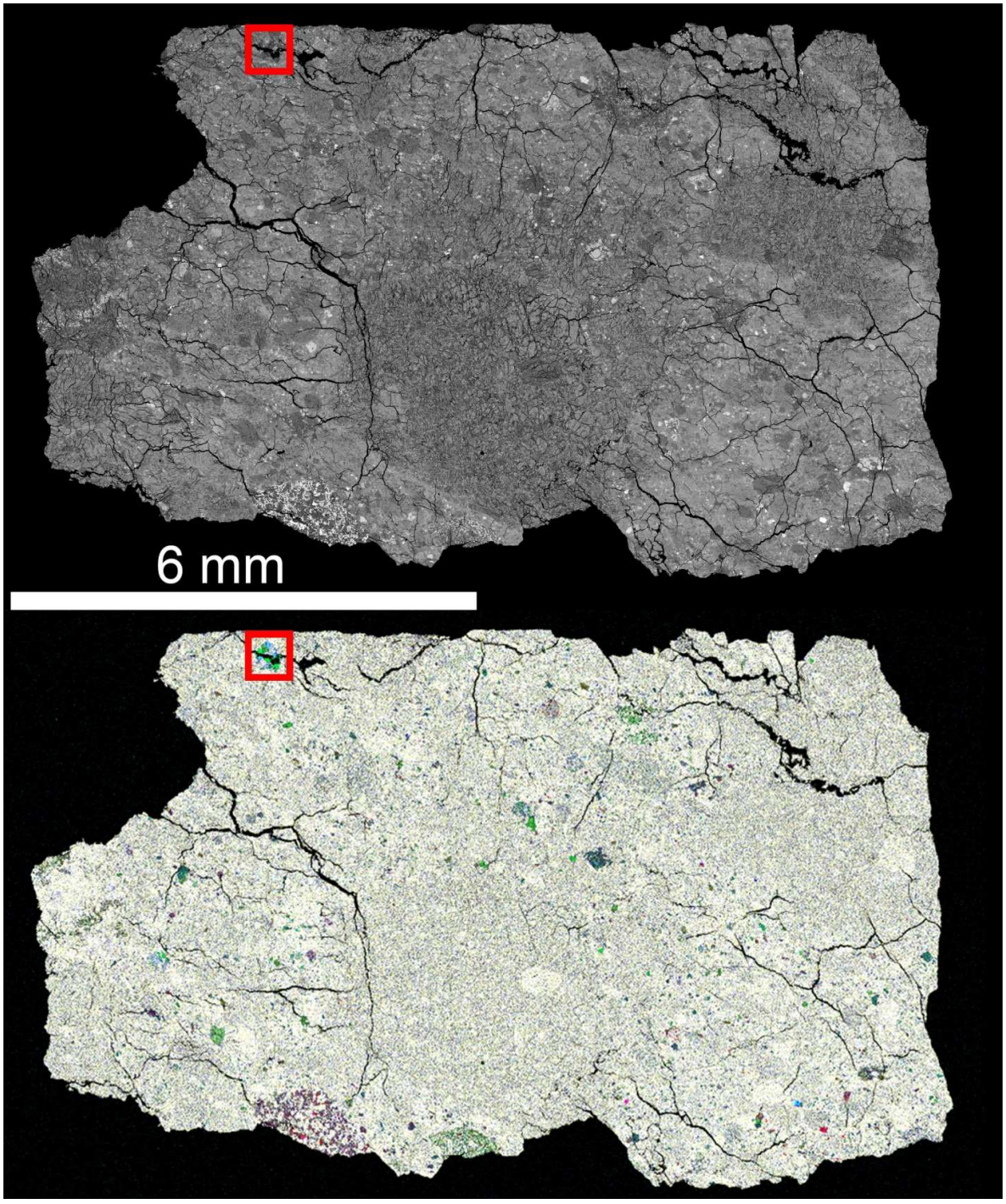

Figure 1.

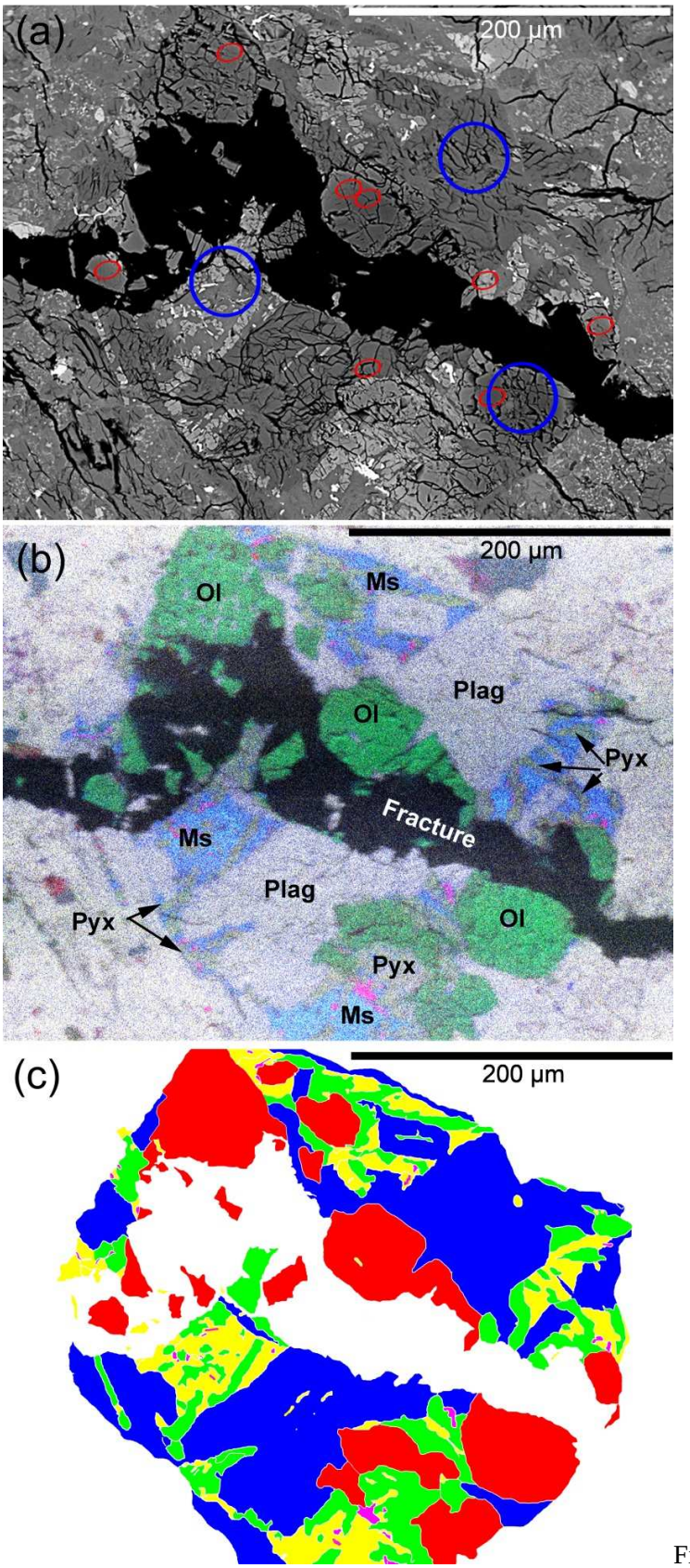
(a)
200 µm
(b)
200 µm
Ol
Ms
Plag
Ol
Pyx
Fracture
Ms
Plag
Pyx
Ol
Pyx
Ms
(c)
200 µm

912 Figure 2.

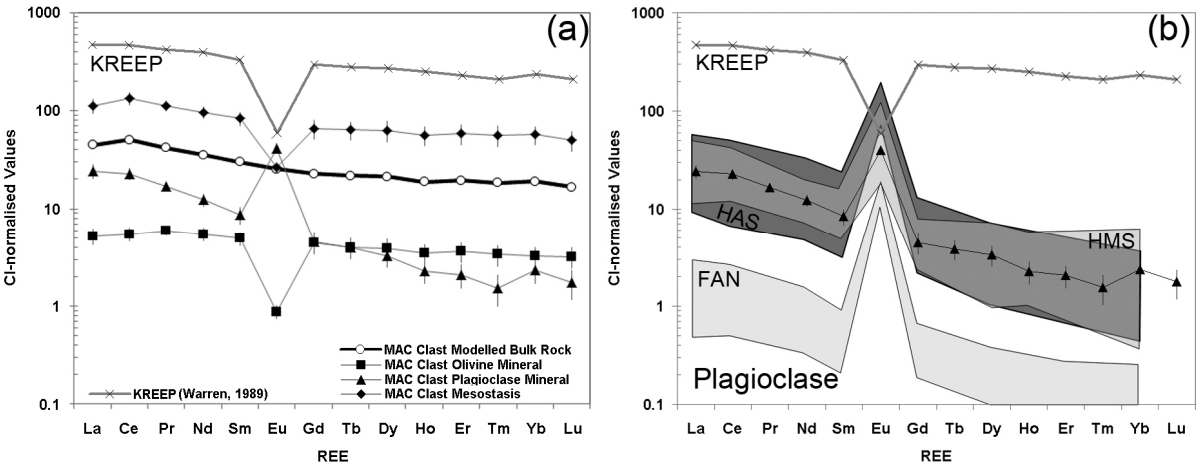

913

914 Figure 3.

915

916

917

918

919

920

921

922

923

924

925

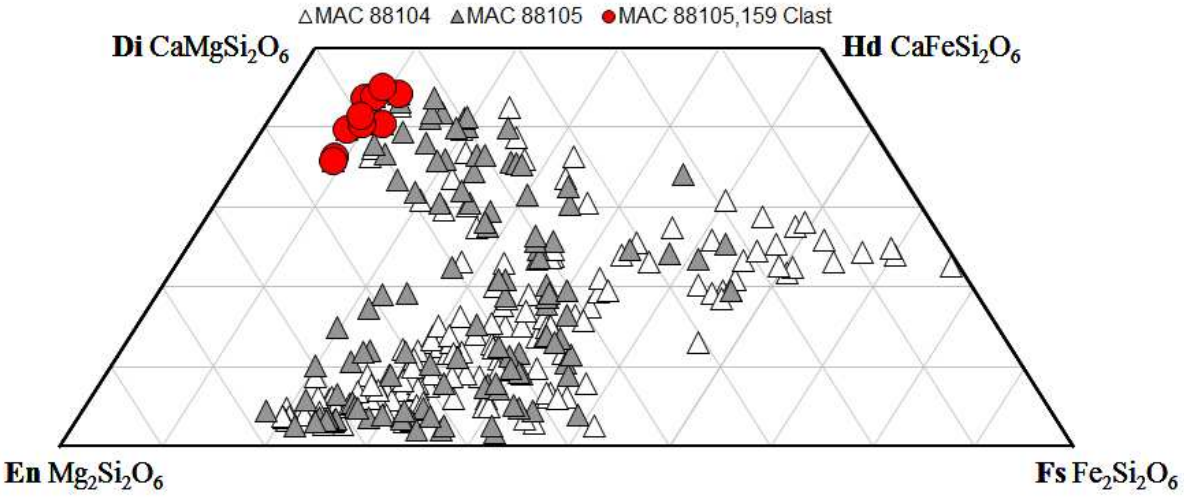
△MAC 88104 △MAC 88105 ●MAC 88105,159 Clast
Di CaMgSi2O6
Hd CaFeSi2O6
En Mg2Si2O6
Fs Fe2Si2O6

Figure 4.

943

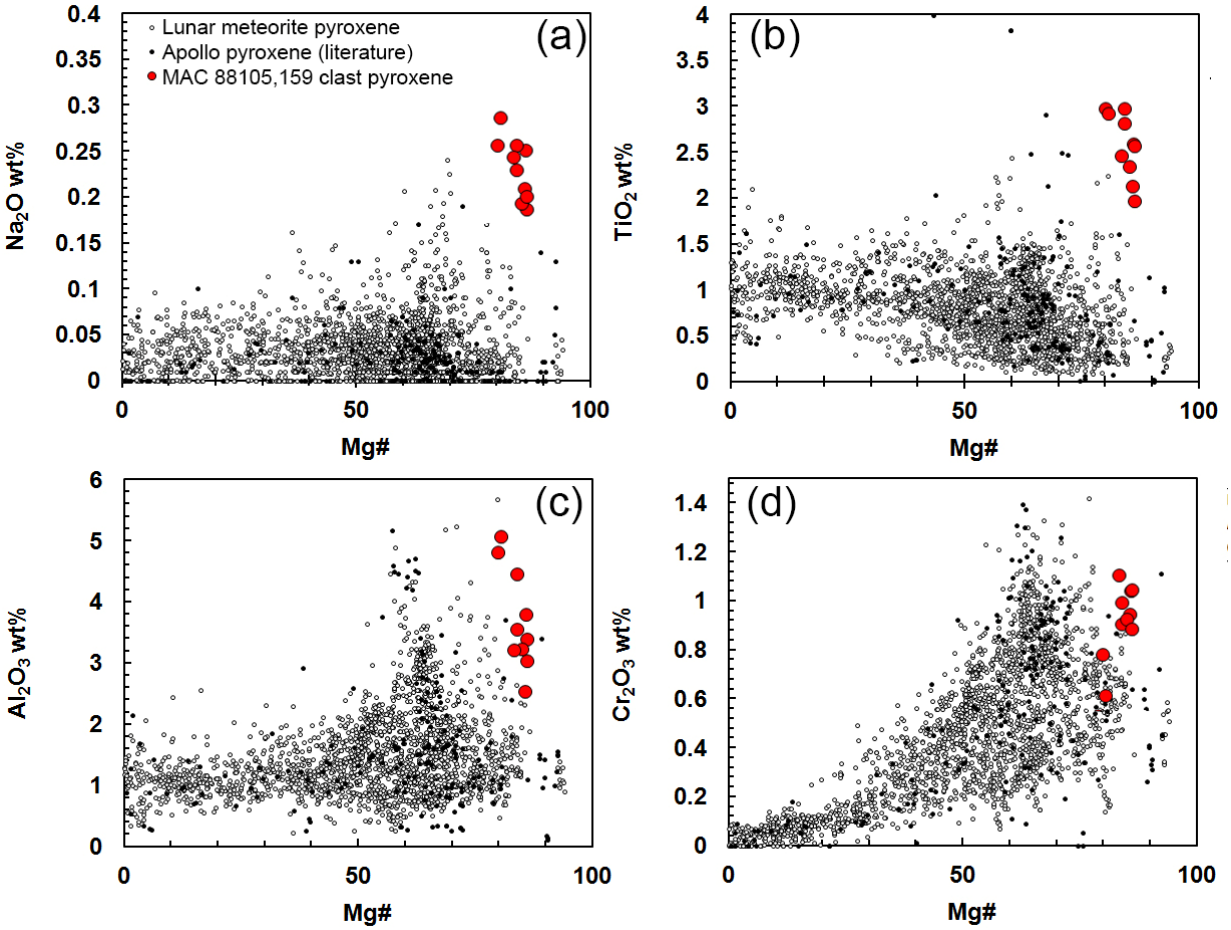

944
945 Figure 5.

946

947

948

949

950

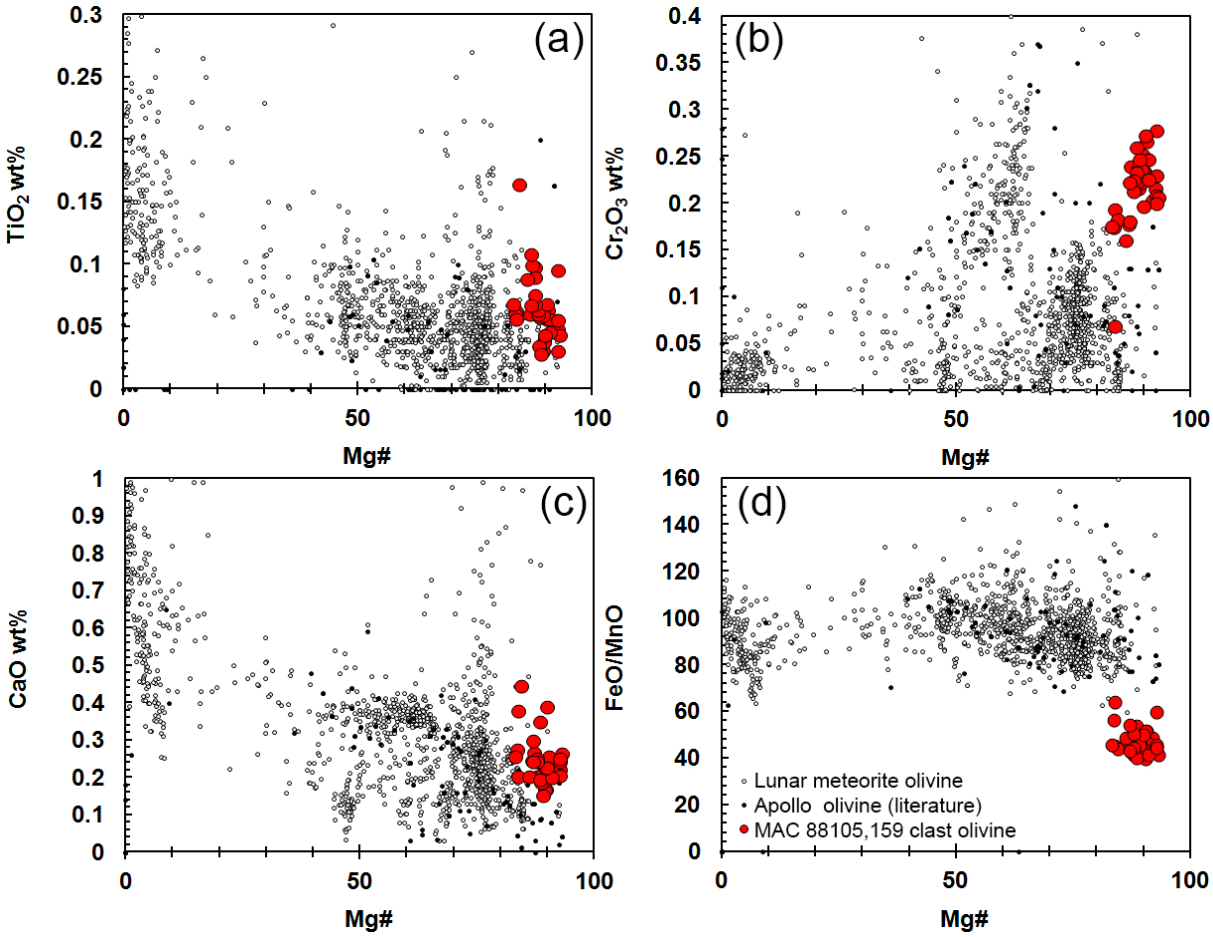
(a)
(b)
(c)
(d)
TiO2 wt%
Cr2O3 wt%
CaO wt%
FeO/MnO
Mg#
Lunar meteorite olivine
Apollo olivine (literature)
MAC 88105,159 clast olivine

Figure 6.

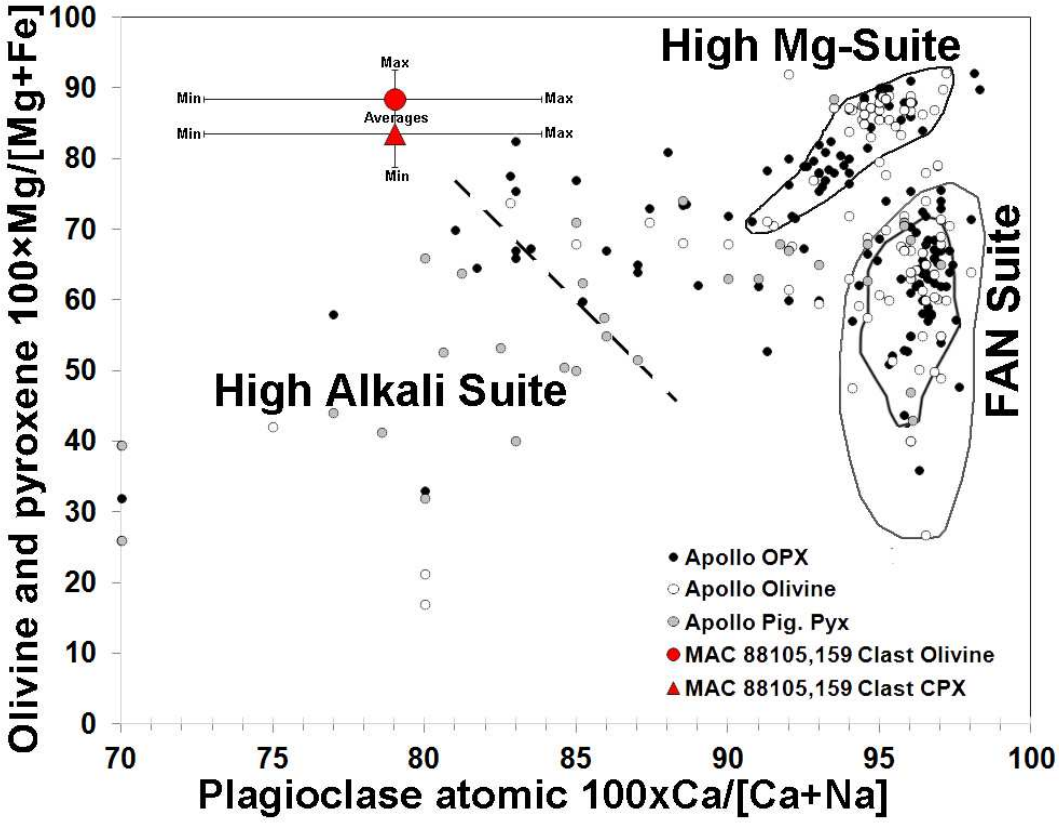
High Mg-Suite
High Alkali Suite
FAN Suite
Max
Min
Max
Averages
Min
Max
Min
Apollo OPX
Apollo Olivine
Apollo Pig. Pyx
MAC 88105,159 Clast Olivine
MAC 88105,159 Clast CPX
Olivine and pyroxene 100×Mg/[Mg+Fe]
Plagioclase atomic 100xCa/[Ca+Na]
0
10
20
30
40
50
60
70
80
90
100
70
75
80
85
90
95
100

Figure 7.

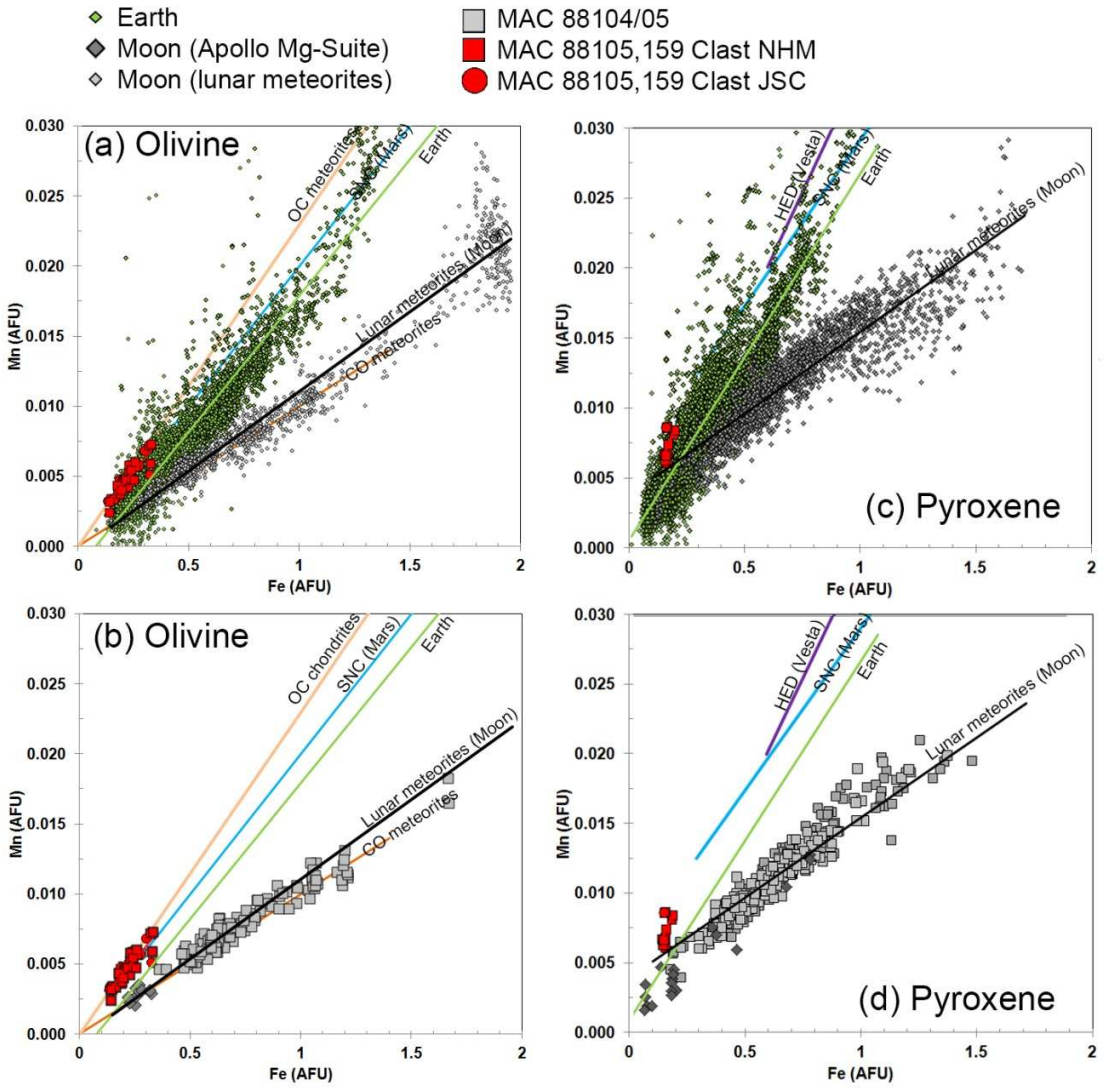

967

968 Figure 8.

969

970

971

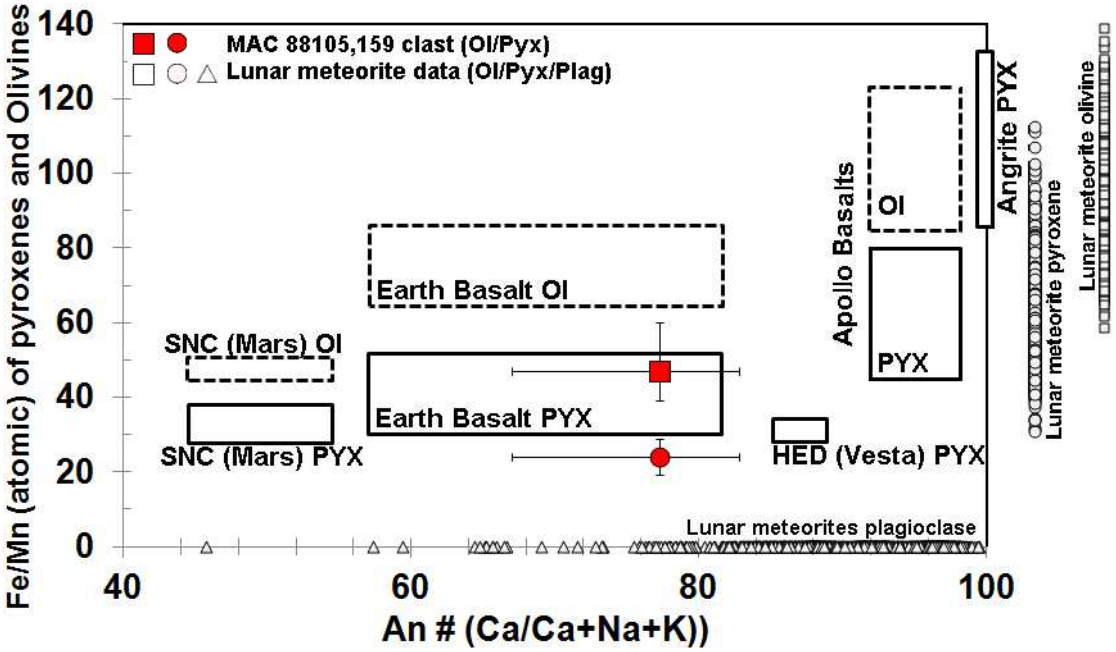
MAC 88105,159 clast (Ol/Pyx)
Lunar meteorite data (Ol/Pyx/Plag)
Fe/Mn (atomic) of pyroxenes and Olivines
An # (Ca/Ca+Na+K))
Earth Basalt Ol
SNC (Mars) Ol
Earth Basalt PYX
SNC (Mars) PYX
HED (Vesta) PYX
Apollo Basalts
Ol
PYX
Angrite PYX
Lunar meteorite olivine
Lunar meteorite pyroxene
Lunar meteorites plagioclase

Figure 9.

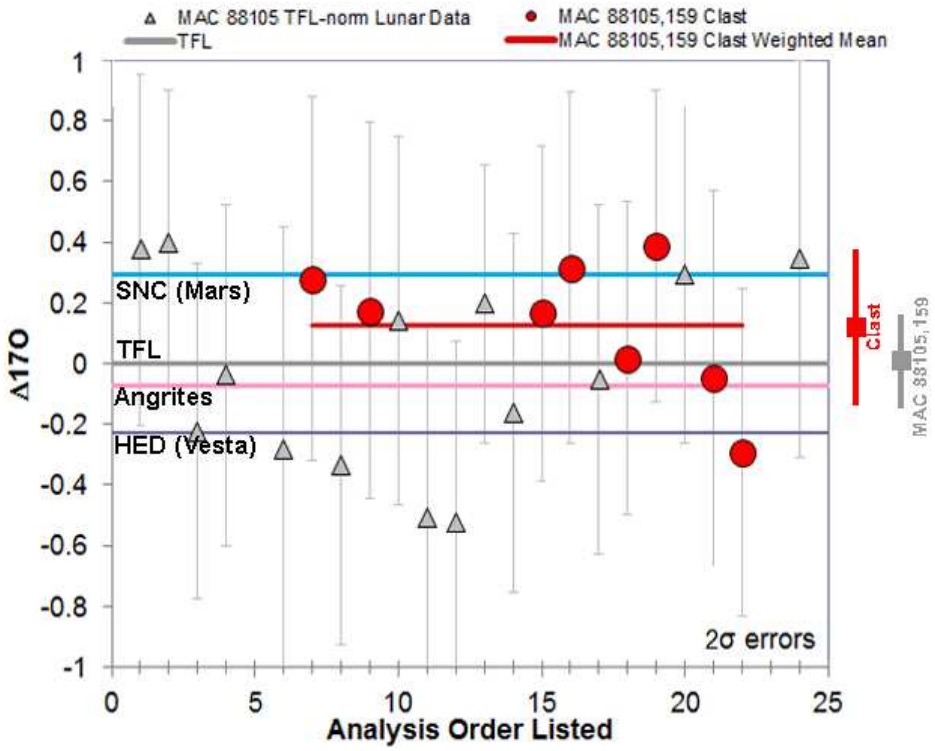
MAC 88105 TFL-norm Lunar Data
TFL
MAC 88105,159 Clast
MAC 88105,159 Clast Weighted Mean
SNC (Mars)
TFL
Angrites
HED (Vesta)
2σ errors
Δ17O
Analysis Order Listed
Clast
MAC 88105,159

Figure 10.